Analysis Thermal Behavior of a Locally Heated Solar Chimney

Aguilar-Castro, K. M. [1]*, Macias-Melo, E. V. [2], Torres-Aguilar, C. E. [3]

[1] *Universidad Juárez Autónoma de Tabasco, División Académica de Ingeniería y Arquitectura (DAIA-UJAT), Carretera Cunduacán-Jalpa de Méndez, km. 1, Cunduacán, Tabasco, CP 86690, México. karla.aguilar@ujat.mx*

[2, 3] *Universidad Juárez Autónoma de Tabasco, División Académica de Ingeniería y Arquitectura (DAIA-UJAT), Carretera Cunduacán-Jalpa de Méndez, km. 1, Cunduacán, Tabasco, CP 86690, México.*

Abstract: This paper presents the thermal behavior of a partially heated solar chimney under hot-humid climate conditions. The solar chimney (SCH) is 2 m high and 0.8 m wide and consists of an absorber plate and a translucent plate. The SCH allows a cavity thickness variation from 0 to 0.28 m, an inclination angle variation from 0 to 90º, and allows varying the amount of energy absorbed by the absorber plate and translucent plate. These plates were heated by resistors, simulating a solar irradiance range of 225 to 900 W/m^2 (absorber plate) and from 12.15 to 50 W/m^2 (translucent plate). Twelve tests were conducted with different configurations varying the power supplied to both plates, the thickness of the absorber plate cavity, and the 90º inclination angle. The variables measured were temperature, air velocity at the inlet, and heat flow on the side walls and rear wall. As a result, a maximum air renewal of 51.43 ACH was obtained, equivalent to the air changes used in a paint booth. The results show that the partially heated solar chimney can be used as a passive ventilation system for air renewal.

Keywords: ACH, Solar chimney, ventilation, buildings.

1. INTRODUCTION

The energy sector of Mexico faces the accelerated growth of energy to satisfy the thermal comfort of residential buildings. According to the “Comisión Nacional para el Uso Eficiente de la Energía” (CONUEE, 2016) [1], 30% of residential energy consumption is addressed to thermal comfort in hot weather zones. The “Secretaría de Energía” from México (SENER, 2017) [2] estimates that 1.76 billion dollars of subsidy were addressed to satisfy the thermal comfort in residential buildings from hot weather zones, which is a problem that must be dealt with reduce negative impacts. A negative impact is the pollution of the environment due to the energy production to satisfy thermal comfort in buildings and the increasing cost of electric services.

Based on ISO 7730 [3], thermal comfort “is a mental condition that expresses the satisfaction with the thermal ambient,” which means that it is necessary to achieve a thermal equilibrium; although the thermal comfort parameters varying respect to every person; the thermal sensitivity is individual although the temperature is between 18 and 26°C. The environmental parameters influencing thermal sensitivity are ambient temperature, relative humidity, solar radiation, and wind velocity.

The thermal comfort in an enclosure is maintained by implementing an active system or a passive system. Active systems work with conventional energy sources. On the other side, passive systems work with renewable energy, and their performance is in the function of the orientation of the building and the integration of passive systems with the façade, for example. Some passive systems implemented in buildings are the Trombe Wall, the Parietodinamyc Wall, the earth-air heat exchanger, and the solar chimneys. The solar chimney is an alternative passive system that induces the ventilation of a building through the constant air renovation to the inside from the outside environment [4]; a solar chimney increases the temperature gradients to induce a temperature change inside the room according to its function and environment condition which permits to achieve thermal comfort.

Furthermore, the study of solar chimney performance is interesting technology of passive systems to provide thermal comfort indoor a building in an ecological form. The use of solar chimneys can reduce the electric energy consumption of conventional methods. The use of solar chimneys contributes to reducing the emissions of pollutants. Solar chimneys can be used on the roof, façade, or in combination with tilt.

Recent studies of solar chimneys have focused on obtaining the highest efficiency levels of velocity or air renovation and temperature gradient increases. Theoretical studies [5]-[7], experimental studies [8][9], and theoretical-experimental studies [10] evaluated the importance of parameter as channel height, tilt, cavity area, and solar radiation and how these parameters influence directly or indirectly in the solar chimney performance [10]-[12]. The revised studies revealed the anomalies in the airflow behavior in the output of solar chimneys where air counterflow formed a tampon. Therefore, it is necessary to study the performance of airflow in the output varying the solar radiation in different solar chimney sections through experimental tests and determine the speed of air renovation and temperature gradients.

2. MATERIALS AND METHODS

A. Mathematical model

The heat flux (q_w) through the wall is determined by applying Fourier's Law (1):

$$q_w = \lambda \, \mathrm{A_w} \frac{\Delta \mathrm{T}}{\mathrm{L}} \tag{1}$$

where λ is the thermal conductivity of the insulating material, A_w is the total area of the insulating material, ΔT is the temperature difference between the sides of the insulating material, and L is the thickness of the insulating material.

The heat flow through the translucent-simulated plate (TSP) is determined by Equation (2). The thermal resistance of the translucent plate is neglected since it is a thin material. Furthermore, the value of the convective-radiative coefficients is the same on both sides of the translucent material.

$$q_{TSP} = h\mathrm{A}_{TSP}\left(\mathrm{T}_{TSP} - \mathrm{T}_{\mathrm{in}}\right) \tag{2}$$

where h is the convective heat transfer coefficient, A_{TSP} is the area of the translucent plate, T_{TSP} is the temperature in the translucent plate, and T_{in} is the inlet air temperature.

Equation (3) represents the heat flux removed by the air, where the absorber energy by TSP; this energy is divided into inside and outside components. Therefore, the system energy balance is calculated through Equation (4).

$$q_{air} = P_{AP} - q_{ws} + P_{TSP} - q_{TSP} \tag{3}$$

$$P_{AP} + P_{TSP} - q_{ws} - q_{TSP} = \dot{m}Cp\left(\mathrm{T}_{out} - \mathrm{T}_{in}\right) \tag{4}$$

where $\dot{m}$ is the mass flow inside the cavity, and Cp is the specific heat evaluated at the mean temperature between the inlet (T_{in}) and outlet (T_{out}).

The thermal efficiency for the SCH can be determined by Equation (5) [13], where A_{AP} is the area of the absorber plate.

$$\eta = \left(\frac{\dot{m}Cp(\mathrm{T}_{out} - \mathrm{T}_{in})}{(\mathrm{P}_{AP} + \mathrm{P}_{TSP})\mathrm{A}_{AP}}\right) \times 100 \tag{5}$$

Equation (6) expressed the air changes per hour (ACH) to analyze the airflow, where $\dot{\mathrm{V}}$ is the volumetric flow and W is the volume of the enclosure or room. The ACH value indicates the ventilation level of a sector and analyzes the air quality.

$$\mathrm{ACH} = \frac{\dot{\mathrm{V}}}{\mathrm{W}} \tag{6}$$

B. Design and construction

Fig. 1 shows the dimensions of the solar chimney (SCH). The channel height and width are 2 m and 0.8, respectively; the SCH comprises of an absorber plate (AP) and a translucent-simulated plate (TSP). The SCH allows varying the channel thickness from 0 to 0.28 m, the tilt from 0 to 90°, and the absorber energy through the TSP. The plates were heated using thermal resistances, which simulated the solar irradiance from 225 to 900 W/m^2 (absorber plate) and 12.15 to 50 W/m^2 (TSP).

The channel is a space inside composed of four envelopes: front, back, and side walls. The front wall is the TSO, while the back wall is the AP; both envelopes were manufactured using galvanized sheet metal (with a mate black cover), and between the sheets, a distribution of thermal resistance was installed for heating. The side walls were insolated thermally with Foamular (extruded polystyrene) of 0.0508 m (2 in) thickness; the side walls were instrumented with thermopiles to quantify the heat losses. The shell structure of SCH was built with steel profiles, and two bearings coupled to the framework's support were employed for the rotation system.

C. Instrumentation

The side and back walls were instrumented with heat flow transducers, built using T-type thermocouples to quantify heat loss (q_w). Also, the thermopiles were built using T-type thermocouples. The air temperature inside (T_c) the channel at different locations was registered using 12 T-type thermocouples (±0.5°C); the thermocouples were installed to register the air temperature in the hydrodynamic boundary layer over the absorber plate and the center of the channel. The air velocity (v) was measured in the channel inlet using a Delta Ohm hot-wire anemometer, model HD4V3TS2 (±0.06 m/s). The temperature gradients between the inlet and outlet channel (T_{out} - T_{in}) were measured through a thermopile in an arrangement of four points and two PT100 sensors to measure the inlet and outlet temperature of the channel. A sensor AMT1001 was implemented to measure the relative humidity of the channel's inlet. The heating of the TSP (P_{TSP}) and AP (P_{AP}) was induced through the electrical resistances of constantan of 2.66 and 10.67 Ω/m, respectively; the electrical resistances were connected to DC energy source BK PRECISION 1673 and GW INSTEK. A digital multimeter Keysight 34972A was employed as a data acquisition system.

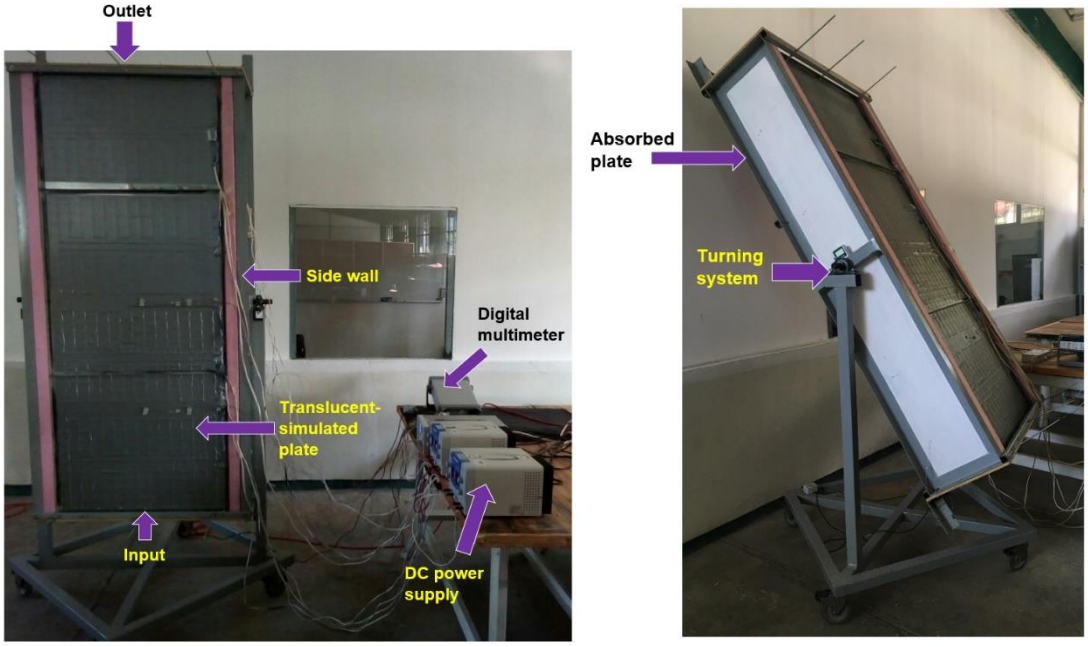

Fig. 1 Experimental setup of SCH.

D. Procedure

Table 1 shows the configurations of the experimental test of SCH. The partially heated was implemented to simulate the shaded conditions over the plate surfaces. The tilt of the prototype was fixed at 90° since this is the tilt to obtain the maximum ACH for the configuration of SCH reported by Villar-Ramos [14].

Table 1. Experimental test

No.	Plate Spacing (m)	P_{AP} (W)	P_{STP} (W)	Angle of inclination (°)	Graphical representation
1	0.075	360	20	90	
2	0.125				
3	0.175				
4	0.075	720	40		
5	0.125				
6	0.175				
7	0.075	1080	60		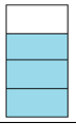
8	0.125				
9	0.175				
10	0.075	1440	80		
11	0.125				
12	0.175				

The experimental tests were executed in the next order:

1. Fixed inlet and outlet area for 0.075 m channel thickness.
2. Fixed heating for AP of 360 W.
3. Fixed heating for STP of 20 W.
4. Fixed tilt of 90°.
5. Activation of sensors and configuration of digital multimeter for recording data.
6. Start the test until the system achieves a steady state.
7. Repeat steps 1 to 6 for 0.125 and 0.175 m thickness.
8. Repeat steps 1 to 7 for other heat flow in the AP and STP.

3. RESULTS AND DISCUSSION

Fig. 2 shows the temperature of the inlet and outlet air temperature of SCH during the transient state until the system achieved the steady state. The shaded zone in Fig. 2 represents the transient zone, while the white zone represents the steady zone. The steady state was observed after one hour of the test approximately. The results correspond to Test 3. The maximum temperature difference was 9.45°C between T_{in} and T_{out}, indicating homogeneous heating inside the solar chimney.

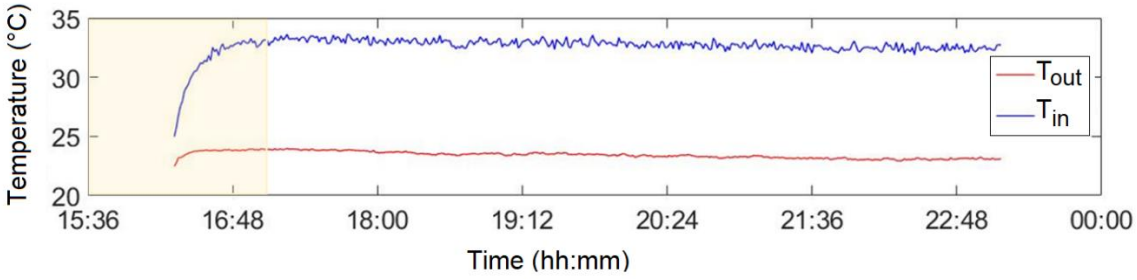

Fig. 2 Temperature behavior during transient state for Test 3

The results of 12 tests during the steady state are concentrated in Table 2. The results presented show that the highest difference between T_{in} and T_{out} was 9.44°C for the configuration with a thickness of 0.075 m with a heat flow

induced in the absorber and translucent plates of 1080 and 60 W, respectively; in this configuration, the highest air velocity was registered of 0.68 m/s. For the configuration of the solar chimney with a thickness of 0.175 m and with the same induced heat flow, the highest air renovation of 51.426 ACH; the efficiency of this configuration was 58.48% which was the highest efficiency recorded. However, the solar chimney efficiencies for the other configurations varied slightly.

The highest temperature of AP was 97.64°C, obtained for a configuration of 1440 and 80 W heat flows supplied to the AP and STP, respectively with a thickness of 0.075 m. Results of Table 2 shows that the AP temperature increased as the supplied heat flow for the different thickness. The heat flow loss by the side walls was minimal compared to P_{AP} and P_{STP}.

The behavior of the parameters during the test is described in the next section to improve the comprehension of the results obtained during the experimental evaluations.

Table 2. Results of experimental tests

No.	d (m)	P_{AP} (W)	P_{STP} (W)	T_{AP} (°C)	T_{STP} (°C)	T_{in} (°C)	T_{out} (°C)	ΔT_{out-in} (°C)	T_c (°C)	q_w (W)	v ($^m/_s$)	$\dot{m}$ ($^{Kg}/_s$)	$\dot{V}$ ($^{m^3}/_h$)	η (%)	**ACH** ($^1/_h$)
1	0.075	360	20	50.35	32.42	28.60	32.16	3.57	31.85	13.93	0.37	0.10	305.56	58.26	11.32
2		720	40	70.65	48.41	30.14	36.66	6.53	34.92	31.32	0.55	0.11	345.21	58.11	12.79
3		1080	60	93.71	44.35	23.48	32.93	9.45	29.31	50.18	0.68	0.11	347.58	57.90	12.87
4		1440	80	97.64	48.07	27.32	36.24	8.92	33.42	63.47	0.55	0.16	500.79	58.08	18.55
5	0.125	360	20	51.86	27.52	24.88	26.47	1.59	25.97	14.27	0.36	0.22	675.31	58.16	25.01
6		720	40	76.79	42.02	25.92	29.77	3.86	28.41	29.51	0.41	0.18	571.24	58.29	21.16
7		1080	60	95.40	46.31	26.77	31.39	4.62	29.78	48.70	0.46	0.23	719.87	58.05	26.66
8		1440	80	96.19	47.11	27.50	32.42	4.92	38.19	60.68	0.48	0.29	909.26	58.25	33.68
9	0.175	360	20	54.01	30.69	27.62	28.64	1.02	28.13	13.81	0.27	0.34	1062.00	58.37	39.33
10		720	40	78.33	44.01	29.42	31.20	1.78	31.12	30.69	0.37	0.39	1248.00	57.96	46.22
11		1080	60	97.59	49.08	30.00	32.46	2.45	32.21	48.85	0.42	0.43	1388.49	58.48	51.43
12		1440	80	96.33	47.89	29.72	33.34	3.63	32.41	60.21	0.47	0.39	1238.72	58.06	45.88

A. Absorber plate temperature (T_{AP})

Fig. 3 shows the temperature of the absorber plate considering the different thicknesses of the channel evaluated. Fig. 3 shows that the influence of different thicknesses in the increasing temperature is minimal; this effect was observed with the temperature registered for the thickness of 0.075, 0.125, and 0.175 m using the same configuration of heat flow of absorber and translucent plate. The obtained results for a heat flow of 360 W were very similar to the data reported by Suárez et al. [15] of 45°C for the TSP.

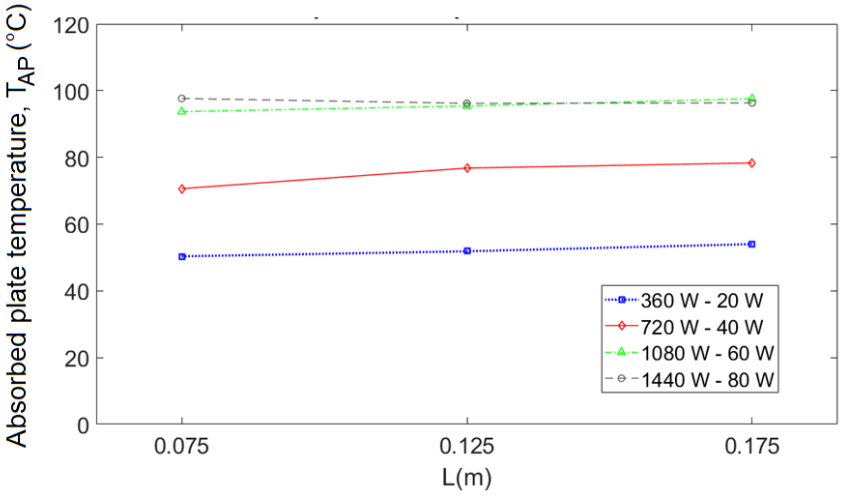

Fig. 3 AP temperature respect to channel tickness

B. Temperature difference between T_{out} and T_{in}

Fig. 4 shows the temperature difference behavior for the different thicknesses of the channel. The highest temperature difference was 9.45°C for the lowest thickness and heat flow of 1080 and 60 W for absorber and translucent plates, respectively. The behavior was similar when the absorber plate was heated from 1080 W to 1440 W with a maximum temperature difference of 0.5°C; this implied that the temperature difference of the system presents minimal changes. The $\Delta T_{out\text{-}in}$ increased as the energy for heating the absorber and translucent plates, and $\Delta T_{out\text{-}in}$ increased as decreased the channel thickness.

C. SCH efficiency

Fig. 5 shows the behavior of SCH efficiency as a function of channel thickness. The lowest efficiency was 57.9% with a channel thickness of 0.075 m and a heat flow of AP and STP of 1080 and 60 W, respectively; the highest efficiency was 58.48% with the same heat flow induced for AP and STP. The obtained efficiency is in the range of values for a traditional SCH (up to 61%) [16]. Fig. 5 shows that the difference in efficiencies is minimal, and their tendency is unclear for channel thickness and heat flows supplied; the efficiencies were from 57 to 59%.

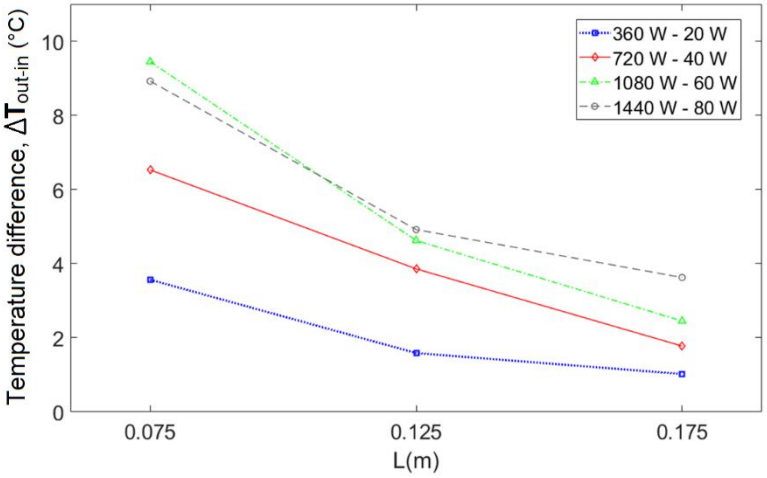

Fig. 4 Temperature difference between inlet and outlet for different channel thickness

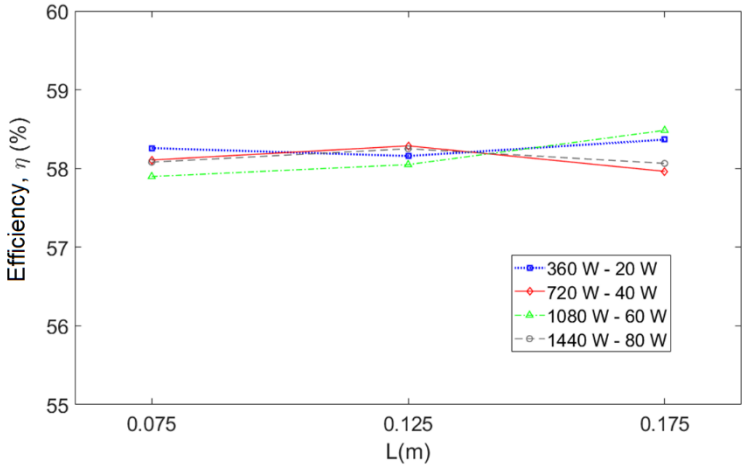

Fig. 5 SCH efficiency for different channel thickness

D. Air changes per hour (ACH)

The results show that the ACH values increased as channel thickness while the influence of heat flow supplied in the ACH induced is minimal. The larger channel thickness permitted to obtain higher ACH, therefore the configuration of channel thickness of 0.075 m permitted to induce between 11 and 18 ACH, between 25 and 33 ACH for the channel thickness of 0.125 m, and between 39 to 51 ACH for the channel thickness of 0.175 m. The results indicated that the

SCH prototype is suitable for providing ventilation in different spaces; for example, for the residential sector, the interval of air renovation is from 15 to 25 ACH, while for the industrial sector, the SCH can be implemented for a paint booth which required from 25 to 50 ACH.

The comparison between the ACH obtained in this study and the values reported by Villar-Ramos [14] shows that the results of SCH with located heated are better than the homogeneous heated when the heat flow supplied is similar. For example, a homogeneous and uniform heat flow of 750 W for AP y 40 W for STP (channel thickness of 0.175 m) induces 12 ACH, lower than the 46 ACH induced by the same configuration with a partially heated. This fact shows that the located heated is more suitable for achieving higher ACH; in addition, that represents a real situation where the vertical wall is heated in a non-homogeneous form due to the sun's movement and the position of the building.

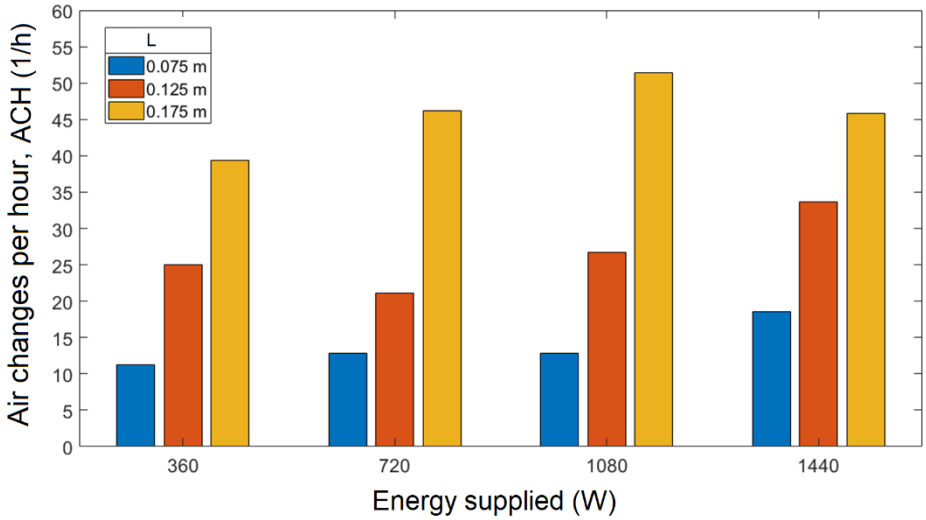

Fig. 6 Air changes per hour vs supplied energy.

4. CONCLUSIONS

In this study the thermal behavior of SCH with located heated was analyzed by varying the solar irradiance in different sections through experimental tests to determine the air renovation and temperature gradients.

- The results of tests revealed that the absorber plate temperature increased as the heat flow was supplied. However, this behavior changed after a heat flow of 1080 W since the changes in absorber plate temperature were minimal. Also, the influence of the channel thickness was minimal with the temperature registered.
- The difference on performance between 1080 W and 14400 W configurations was minimal. Therefore, increasing the heat flow does not improve the performance of SCH.
- The air velocity and the energy removal were increased when the channel thickness was reduced, and the heat flow increased.
- The difference between the efficiency of SCH configurations varying the channel thickness and the heat flow for both plates is ⟨1%. The results show that efficiency depends on the removed and supplied energy. Therefore, the removed energy increases as the supplied heat flow; this tendency was observed with all configurations evaluated.
- The channel thickness influences the air renovation, ACH; therefore, the configuration of the highest channel thickness induced the highest ACH value. Results show that the configuration using a heat flow of 1080 W for the AP was better than that using a heat flow of 1440 W.

In summary, it is concluded that the SCH with located heated is suitable to be used as a ventilation passive system. Evaluating the thermal performance of SHC with partial heating permitted us to determine the feasibility of this system since the experiment simulated shaded conditions and varying solar irradiance.

5. REFERENCES

[1] CONUEE. (2016). Estudio de caracterización del uso de Aire acondicionado en Vivienda de interés social.CONUEE:México.DF

[2] SENER. (2018).Cómo enfrentar el reto de la creciente demanda de confort térmico en México.SENER:Mexico.DF

[3] AENOR. (2006). AENOR - Norma UNE-EN ISO 7730:2006 Ergonomía del ambiente térmico. Determinación analítica e interpretación del bienestar térmico mediante el cálculo de los índices PMV y PPD y los criterios de bienestar térmico local (ISO 7730:2005).Available at: http://www.aenor.es/aenor/normas/normas/fichanorma.asp?codigo=N0037517&tipo=N [Accessed February 19, 2012].

[4] H. Sharon, "A detailed review on sole and hybrid solar chimney based sustainable ventilation, power generation, and potable water production systems", Energy Nexus, vol. 10, pp.100184, 2023.

[5] L. Shia, G. Zhanga, W. Yangb, D. Huangc, X. Chengd, S. Setunge, "Determining the influencing factors on the performance of solar chimney in buildings", Renewable and Sustainable Energy Reviews, vol. 88, pp. 223–238, 2018.

[6] J. Xaman, R. Vargas López, M. Gijón Rivera, I. Zavala Guillen, M. J. Jiménez Arce, "Transient thermal analysis of a solar chimney for buildings with three different types of absorbing materials: Copper plate/PCM/concrete wall", Renewable Energy, vol. 136, pp. 139-158, 2019.

[7] M.A. Esmail, S. Mohammad Raghib, S. Jihad Al, "A Novel Design of Solar Chimney for Cooling Load Reduction and other Applications in Buildings", Energy and Buildings, vol. 153, pp. 219-230, 2017.

[8] W. Rattanongphisata, P. Imkongb, S. Khunkongb, "An Experimental Investigation on the Square Steel Solar Chimney for Building Ventilation Application", Energy Procedia, vol. 138, pp.1165–1170, 2017.

[9] O. Khalil Ahmed, A. Sabah Hussein, "New design of Solar Chimney (Case study)", Case Studies in Thermal Engineering, vol. 11, pp. 105-112, 2018.

[10] H. Hussain Al-Kayiem, K.V. Sreejaya, Aja O. Chikere, "Experimental and numerical analysis of the influence of inlet configuration on the performance of a roof top solar chimney", Energy and Buildings, vol. 159, pp. 89-98, 2018.

[11] Ahmed Abdulnabi Imran, Jalal M. Jalil, Sabah T. Ahmed, "Induced flow for ventilation and cooling by a solar chimney", Renewable Energy, vol. 78, pp. 236-244, 2015.

[12] Casals fans of innovation, (2019), Cómo calcular la renovación por hora según la actividad de un local. Available at: https://www.casals.com/assets/uploads/editor/file/renovacion_de_aire_en_locales_tipicos_casals.pdf

[13] K.S. Ong, C.C. Chow, "Performance of a solar chimney", Sol. Energy, vol. 74, pp. 1–17, 2003.

[14] M.M., Villar Ramos, "Análisis experimental del comportamiento térmico de una chimenea solar de un canal", Universidad Juárez Autónoma de Tabasco, Tabasco, México, 2019.

[15] M.J. Suárez López, A.M. Blanco Marigota, A. J. Gutiérrez Trashorras, J. Pistono Favero, E. Blanco Marigota, "Numerical simulation and exergetic analysis of building ventilation solar chimneys", Energy Conversion and Management, vol. 96, pp. 1–11, 2015.

[16] M. Corcione, L. Fontana, A. Quintino, "First analysis of a novel design of a solar chimney with absorber elements distributed in the air channel", Applied Thermal Engineering, vol. 230, pp. 120539, 2023.

DOI: https://doi.org/10.15379/ijmst.v10i2.2976